Medium-mass nuclei with Δ excitations under compression

Mahmoud A. Hasan,[1,2] James P. Vary,[2,3] and T.-S. H. Lee[4]
[1]*Applied Science University, Amman, Jordan*
[2]*International Institute of Theoretical and Applied Physics, Ames, Iowa 50011*
[3]*Department of Physics and Astronomy, Iowa State University, Ames, Iowa 50011*
[4]*Physics Division, Argonne National Laboratory, Argonne, Illinois 60439*
(Received 16 January 2001; published 2 July 2001)

The ground state properties of ^{90}Zr, ^{100}Sn, and ^{132}Sn at equilibrium and at large amplitude compression are investigated. We use a realistic effective baryon-baryon Hamiltonian that includes N-N, N-Δ, and Δ-Δ interactions. We perform the calculations in no-core model spaces within the framework of the constrained spherical Hartree-Fock approximation. We specifically investigate the sensitivity to the sizes of the nucleon and Δ model spaces. At equilibrium, we find no case of mixing between nucleons and Δ's in our largest model space of eight major nucleon shells plus 16 Δ orbitals. On the contrary, there is mixing in ^{90}Zr, and ^{132}Sn in the smaller model space of seven major nucleon shells plus eight Δ orbitals. Expanding the nucleon model space has a larger effect on reducing the static compression modulus and softening the nuclear equation of state than increasing the number of Δ states. Most of the excitation energy delivered to the system during compression is employed by two nuclei with a neutron excess (i.e., ^{90}Zr, ^{132}Sn) to create massive Δ resonances. On the other hand, in the ^{100}Sn nucleus most of the excitation energy goes to a simple reduction in the binding, suggesting a suppressed role for the Δ states. Under extreme compression, at a density 2–3 times the normal nuclear density, the excitation of nucleons to Δ's increases sharply up to 10% of the total number of constituents. At fixed excitation energy under compression, the number of Δ excitations is not dependent on the number of Δ states over the range studied. The Δ-excitation results are consistent with heavy-ion collision data, and suggest an important mean field mechanism for subthreshold pion production in particle-nucleus and nucleus-nucleus collisions.

DOI: 10.1103/PhysRevC.64.024306 PACS number(s): 21.60.Cs, 21.30.−x, 21.60.Jz

I. INTRODUCTION

For many years there has been increasing interest in Δ isobars as constituents of the nucleus together with nucleons. This interest stems from the need to account for the discrepancies between theoretical estimates and experimental measurements of several nuclear properties such as Gamow-Teller strength distributions at low energies. In addition, the contribution of the Δ's to nuclear properties naturally becomes more pronounced with an increase in the collision energy. With the advent of high-precision experiments at intermediate and high energies using electromagnetic and heavy-ion beams, the contribution of the Δ resonances to the structure of nuclei in their ground state and under compression became a major theoretical question [1,2]. Nucleons may no longer be treated as elementary structureless particles. Therefore, the internal dynamics of the nucleons has to be taken into consideration. One method, which incorporates the dynamics associated with the structure of the nucleons in the nuclear system, is to consider the excitations of the nucleon into Δ isobars. In some heavy-ion collision experiments [3,4] the Δ's may constitute up to 10% of the nuclear constituents when the system is compressed.

We have investigated [5–7] the role of the Δ's in several closed shell and closed subshell nuclei: namely, ^{16}O, ^{40}Ca, ^{56}Ni, ^{90}Zr, ^{100}Sn, and ^{132}Sn. Recently [8], we investigated the effect of neutron excess on Δ formation in the exotic nuclei ^{28}O, ^{60}Ca, and ^{70}Ca. At equilibrium, we found that nucleons and Δ's mix only in nuclei that have a neutron excess. By applying a static load the population of the Δ orbitals increases sharply with compression.

In the present work we incorporate larger spaces with realistic effective Hamiltonians in order to improve the treatment of the Δ's and their effect on nuclear properties. Specifically, we expand the size of the model space to eight major oscillator shells (36 orbitals each for neutrons and protons) and increase the number of Δ states to 16 Δ orbitals. In our previous work [5–8] we have used smaller model spaces of varying sizes up to seven major nucleon shells and eight Δ orbitals. In addition, we follow our recent efforts [5,8] and adopt a realistic effective Hamiltonian H_{eff} which contains nucleon-nucleon (N-N), nucleon-Δ (N-Δ), and Δ-Δ interactions and evaluate the effective baryon-baryon interactions using the Brueckner G-matrix [9,10] method.

In our earlier work [6,7] the effective baryon-baryon interactions have been evaluated using the Brueckner G-matrix method only for the N-N potential. That is, the matrix elements associated with the Δ's [11] were evaluated directly from a potential model. Therefore, the Brueckner-type N-Δ correlation effects were not included in the calculations. Here and elsewhere [5,8], this deficiency is removed by using the method developed in Ref. [12]. We define the effective interaction from the G-matrix elements. The G-matrix elements are generated from a coupled-channel $NN \oplus N\Delta \oplus \pi NN$ model [13–15] that was constrained by the data of both the NN elastic scattering and the $NN \rightarrow N\Delta \rightarrow \pi NN$ reaction. Therefore, the strength for the NN to $N\Delta$ transition, a crucial element in predicting the Δ component in nuclei, is under better control than that of the potential model [11] in Refs. [6,7] where the N-Δ and Δ-Δ interactions have been

incorporated in their ''bare'' form.

In the present work, we employ the recent Nijmegen (Nijm.II) local potential [16] for the *N-N* interaction. This potential was fitted to the world *N-N* scattering data with a nearly optimal χ^2 per degree of freedom (1.03 per datum). In our earlier studies [7] we have used the Reid soft-core (RSC) potential [17]. As in previous practices, we adjust the effective interactions in simple ways to reproduce the known equilibrium ground state properties in the spherical Hartree-Fock method.

We anticipate that by investigating the role of the Δ's in nuclei we may better understand intermediate-energy collision processes in which highly energetic heavy nuclei collide and penetrate each other. At suitable energies and with appropriate projectile-target combinations, these collisions can result in the formation of dense nuclear matter 2–3 times higher than the normal nuclear density. The nuclei we investigate here may be viewed as representative of some of the intermediate systems formed in such heavy-ion collisions, again depending on the projectile-target combinations. In addition, by investigating Δ formation under compression, our approach could provide insight into a bulk (mean field) mechanism for ''subthreshold'' pion production processes.

In what follows, we present results for the ground state energies, number of Δ's formed, single-particle (s.p.) energies, and matter densities for ^{90}Zr, ^{100}Sn, and ^{132}Sn at equilibrium and under large compression. The framework is the radial constrained spherical Hartree-Fock (CSHF) approximation. In Sec. II we give a review of the effective Hamiltonian H_{eff} and the model space used in these calculations. In Sec. III we summarize our procedure and strategy. Results and a discussion are presented in Sec. IV.

II. EFFECTIVE NO-CORE HAMILTONIAN H_{eff} AND THE MODEL SPACE

For a nuclear system of A baryons (nucleons of mass m, spin $s=1/2$, and isospin $t=1/2$ and Δ baryons of mass M, spin $s=3/2$, and isospin $t=3/2$) the intrinsic operator can be written as

$$H = T - T_{\text{c.m.}} + V^{BB'} + V_C, \tag{1}$$

where T is the s.p. mass and kinetic energy term, $T_{\text{c.m.}}$ is the center-of-mass kinetic energy, and $V^{BB'}$ is the strong two-baryon interaction operator given by

$$V^{BB'} = V^{NN\leftrightarrow NN} + V^{NN\leftrightarrow N\Delta} + V^{N\Delta\leftrightarrow N\Delta} + V^{N\Delta\leftrightarrow \Delta N} + V^{N\Delta\leftrightarrow \Delta\Delta} + V^{NN\leftrightarrow \Delta\Delta} + V^{\Delta\Delta\leftrightarrow\Delta\Delta}. \tag{2}$$

The last six terms in Eq. (2) represent all possible transition potentials.

In our earlier work [6,7], we have included all possible transitions. Lately, we have neglected the last four channels of the transition potentials, anticipating that most of the contribution to Δ excitations comes from the first two channels, that is, from $V^{NN\leftrightarrow N\Delta}$, and $V^{N\Delta\leftrightarrow N\Delta}$. We continue to neglect these channels in the enlarged model spaces of the present work. V_c is the two-particle Coulomb interaction. We define

$$T_{rel} = T - T_{\text{c.m.}}, \tag{3}$$

with

$$T = \sum_{i=1}^{A} \left[\left(\frac{p_i^2}{2m} + m \right) \Lambda_i^{1/2} + \left(\frac{p_i^2}{2M} + M \right) \Lambda_i^{3/2} \right] \tag{4}$$

and

$$T_{\text{c.m.}} = \frac{P_{\text{c.m.}}^2}{2M_A} = \frac{1}{A} \sum_{ij} \frac{\mathbf{p}_i \cdot \mathbf{p}_j}{2m}, \tag{5}$$

where $\mathbf{p}_i$ is the s.p. momentum operator, and Λ^τ is a s.p. isospin projection operator defined as

$$\Lambda^\tau |\tau'\rangle = \delta_{\tau\tau'} |\tau'\rangle, \tag{6}$$

$$\Lambda^{1/2} + \Lambda^{3/2} = 1. \tag{7}$$

The intrinsic mass operator H can be written

$$H = H_1(\text{one body}) + H_2(\text{two body}), \tag{8}$$

where

$$H_1 = \sum_{i=1}^{A} \left[\frac{p_i^2}{2M} \left(\frac{m-M}{m} \right) + (M-m) \right] \Lambda_i^{3/2} \tag{9}$$

and

$$H_2 = T_{rel} + V^{BB'} + V_C, \tag{10}$$

where

$$[T_{rel}(m)]_{i,j} = \frac{(\mathbf{p}_i - \mathbf{p}_j)^2}{2mA} \tag{11}$$

is the relative kinetic energy operator. In this manipulation we eliminate the center-of-mass kinetic energy in favor of the relative kinetic energy. In Eq. (5), M_A is the total mass of the nuclear system. In general M_A is state dependent, but we approximate $M_A = Am$ and neglect binding energy effects in the kinetic energy operator. The term H_1 serves as a correction and gives a nonzero contribution when it acts on many-body states with Δ components. States with Δ components are said to comprise the Δ sector. H_1 arises solely due to the mass difference between the nucleon and the Δ.

In principle, if one solves the Schrödinger equation in the full infinite Hilbert space of all possible N and Δ many-body configurations, then one gets the exact solution. Technically, this is not feasible beyond light nuclei ($A>4$). Therefore, we truncate the infinite Hilbert space and define an effective Hamiltonian H_{eff} to be used in the truncated model space; hence, $V^{BB'}$ in Eq. (10) becomes $V_{eff}^{BB'}$ and Eq. (10) reads

$$H_2(\text{two body}) = T_{rel}(m) + V_{eff}^{BB'} + V_C. \tag{12}$$

By applying the variational principle, Hartree-Fock equations for N and Δ orbitals can be derived from the effective Hamiltonian within the chosen model space. The compres-

sion of nuclei is achieved by imposing a static load with a radial r^2 constraint. For details see Ref. [6].

The matrix elements of the effective baryon-baryon interaction have been calculated using the Brueckner *G*-matrix method. The effective *N*-*N* interaction is the sum of the Brueckner *G* matrix and the lowest-order folded diagram [18] (second order in *G*) acting between pairs of nucleons in a no-core [18] model space based on the Nijmegen (Nijm.II) potential [16]. The effective interactions associated with the Δ's are evaluated according to the method developed in Ref. [12]. The *G*-matrix elements are generated from a coupled-channel $NN \oplus N\Delta \oplus \pi NN$ model [13–15] that was constrained by the data of both the *NN* elastic scattering and the $NN \rightarrow N\Delta \rightarrow \pi NN$ reaction up to 1 GeV.

The procedure and strategy for evaluating nuclear properties from a defined Hamiltonian, which we follow here, are the same as Refs. [5–8].

We view the constructed effective Hamiltonian in the many-body problem to consist of four sectors with matrix elements as follows:

(i) *N*-*N* sector:

$$\langle T_{rel}(m)\rangle + \langle V_{eff}^{NN}\rangle + \langle V_C^{pp}\rangle.$$

(ii) *N*-Δ sector:

$$\langle V_{eff}^{N\Delta}\rangle + \langle V_C^{p\Delta^+}\rangle.$$

(iii) Δ-*N* sector:

$$\langle V_{eff}^{\Delta N}\rangle + \langle V_C^{\Delta^+ p}\rangle.$$

(iv) Δ-Δ sector:

$$\langle H_1(\text{one body})\rangle + \langle T_{rel}(m)\rangle + \langle V_{eff}^{\Delta\Delta}\rangle + \langle V_C^{\Delta^+\Delta^+}\rangle.$$

We develop our complete H_{eff} in a sequence of steps. First, for the *N*-*N* sector [sector (i)] we evaluate H_{eff} in just the lowest six major oscillator shells, i.e., 21 nucleon orbitals with fixed *n*, *l*, and total angular momentum *j* for the neutrons and for the protons. For the Δ orbitals we use the following 16-oscillator states: $0S_{3/2}$, $0P_{1/2}$, $0P_{3/2}$, $0P_{5/2}$, $1S_{3/2}$, $1P_{1/2}$, $1P_{3/2}$, $1P_{5/2}$, $0D_{1/2}$, $0D_{3/2}$, $0D_{5/2}$, $0D_{7/2}$, $0F_{3/2}$, $0F_{5/2}$, $0F_{7/2}$, and $0F_{9/2}$. Second, we follow our earlier works [6,7] and expand the nucleon model space since we found this necessary to achieve model-space-independent results with increased compression. In keeping with our present goal to investigate the role of the Δ components under large compression we have included a phenomenological extension of the seventh and the eighth major nucleon oscillator shells in our model space. Therefore, the total number of baryon states of specified $(nlsj)$ is 52 (i.e., 36 nucleon orbitals plus 16 Δorbitals). Matrix elements involving nucleons in the first six shells are given by effective Hamiltonians defined above while nucleons in the seventh and the eighth shells are governed by a simple s.p. Hamiltonian

$$h = t + U(r) + U_C, \tag{13}$$

TABLE I. The oscillator energy $\hbar\Omega'$ and the strength parameters λ_t and λ_v used to adjust T_{rel} and V_{eff}^{NN}, respectively, to fit E_{HF} and $r_{\rm rms}$ for each nucleus to the nuclear binding energy (E_{BE}) and nuclear rms radius ($r_{\rm rms}$). The *N*-*N* interaction used in these calculations is the Nijmegen (Nijm.II) potential. The *N*-only calculations are performed in a model space of eight major oscillator shells. The nuclear ground state energies ($E_{\rm g.s.}$) [and the nuclear radius ($r_{\rm rms}$)] that we fit are −784 MeV (4.26 fm), −826 MeV (5.10 fm), and −1104 MeV (5.63 fm) for ^{90}Zr, ^{100}Sn, and ^{132}Sn, respectively.

Nucleus	$\hbar\Omega'$ (MeV)	λ_t	λ_v
^{90}Zr	7.87	1.00	0.977
^{100}Sn	5.30	0.998	1.141
^{132}Sn	4.88	0.999	1.206

where *t* is the s.p. kinetic energy, $U(r)$ is the Woods-Saxon potential given by

$$U(r) = \frac{U_0}{1+\exp\left(\dfrac{r-R}{a}\right)}, \tag{14}$$

where $U_0 = -60$ MeV, $a = 0.6$ fm, and $R = 1.1A^{1/3}$ fm, and U_c is the Coulomb potential of a uniform charge sphere of radius *R*. In order to achieve a smooth matching of the added s.p. states to the self-consistent states of the HF spectrum an additional overall shift of 20 MeV is added to the oscillator diagonal terms of the phenomenological Hamiltonian. This shift is due to the fact that the relative kinetic energy operator is utilized for the lowest six oscillator shells while a pure one-body kinetic energy is used for the higher oscillator shells. For more details see Ref. [19]. This completes the outline of the dynamical model which we use in these calculations.

III. CALCULATIONAL PROCEDURE AND STRATEGY

The matrix elements of the two-body part in the *N*-*N* sector of effective Hamiltonian H_{eff} have been calculated in an oscillator basis consisting of the lowest six oscillator shells with $\hbar\Omega = 14$ MeV and a *G*-matrix starting energy $\omega = 9$ MeV. We follow our established procedure of Refs. [5–8,18,20] to adjust the two-body matrix elements in the *N*-*N* sector to fit the Hartree-Fock energy (E_{HF}) and the root mean square radius ($r_{\rm rms}$) to the nuclear binding energy and the nuclear radius. Therefore, we introduced the adjustable parameters λ_t and λ_v to modify the strength of the matrix elements of T_{rel}, and V_{eff}, respectively. We also scale the two-body matrix elements in the *N*-*N* sector to an optimal value of $\hbar\Omega'$, the oscillator energy.

A separate fit for λ_t, λ_v, and $\hbar\Omega'$ is achieved for each nucleus in each model space with the Δ channels excluded (for more details see Refs. [5–8,18,20]). Nuclear ground state energies and nuclear radii to which we fit the E_{HF} and $r_{\rm rms}$ are −784 MeV, 4.26 fm, −826 MeV, 5.10 fm, −1104 MeV, and 5.63 fm for ^{90}Zr, ^{100}Sn, and ^{132}Sn, respectively. Values of the parameters λ_t, λ_v, and $\hbar\Omega'$ used in these calculations are given in Table I. We then apply the

static load (r^2 constraint) to compress the nucleus. Finally, we activate the Δ channels and apply the static load again to compress the nucleus.

Usually, if some Δ's appear at equilibrium once the Δ channels are activated, we then adjust the fitting parameters in order to ensure the same starting point (the same E_{HF} and the same $r_{\rm rms}$) before applying the static load. For the nuclei of the present study we found no mixing between nucleons and Δ's at equilibrium in the largest model space while ^{90}Zr and ^{132}Sn do exhibit such a mixing in the ground state in a smaller model space.

These calculations are performed in a no-core model space containing a total of 52 baryon states as described above for each baryon isospin channel. We allow for transitions from the 36 nucleon orbitals to the 16 Δ orbitals within the limits of SHF theory. We work in a good T_z scheme where, on the one hand, neutrons and Δ^0 are allowed to mix and, on the other hand, protons mix with Δ^+. The number of baryonic degrees of freedom, including magnetic substates, is 320 s.p. states (240 nucleon states and 80 Δ s.p. states) for each $T_z=+1/2,-1/2$ value for an overall total of 640 states.

IV. RESULTS AND DISCUSSION

We begin by introducing labels for our model spaces: we refer to the model space of seven major oscillator shells (excluding $l>5$) (that is, 26 nucleon states) as the ''7 space'' and the model space consisting of the 7 space plus eight Δ states as ''space I.'' We refer to the model space of eight major oscillator shells (that is, 36 nucleon states) as the ''8 space'' and the model space of the 8 space plus 16 Δ states as ''space II.'' For convenience of presentation we will characterize the compression in terms of the mean radius $r_{\rm rms}$ of the nuclear volume.

We first present the results for ^{90}Zr. The only difference between the results obtained here and those in Ref. [5] (also shown here for comparison) is the size of the nucleon model space and the number of the Δ orbitals included. Here, we employ space II, while the results of Ref. [5] were obtained using space I. The many-body approach, underlying interactions, effective Hamiltonian, and parameter adjustment procedure for ^{90}Zr are the same as those in Ref. [5]. It is worth mentioning that at equilibrium in ^{90}Zr, there is a small amount of Δ present [5] using space I, while using space II we find no mixing between nucleon states and the Δ states. The Δ presence in the ground state drops out in spite of the large increase in the number of delta states in space II relative to space I. One concludes from this that the presence or absence of a trace amount of Δ's at equilibrium in ^{90}Zr is sensitive to the model space selection and, possibly, to other ingredients in the approach.

To see the role of the Δ in determining the equation of state, we show in Fig. 1 the dependence of the calculated Hartree-Fock energy E_{HF} on the compression characterized by the root mean square radius $r_{\rm rms}$. Here we show the results from using four different model spaces. It is seen that near equilibrium ($r_{\rm rms}\sim 4.25$ fm), all curves agree. This indicates that our results for the systems which are close to the nuclear ground state are rather independent of the considered

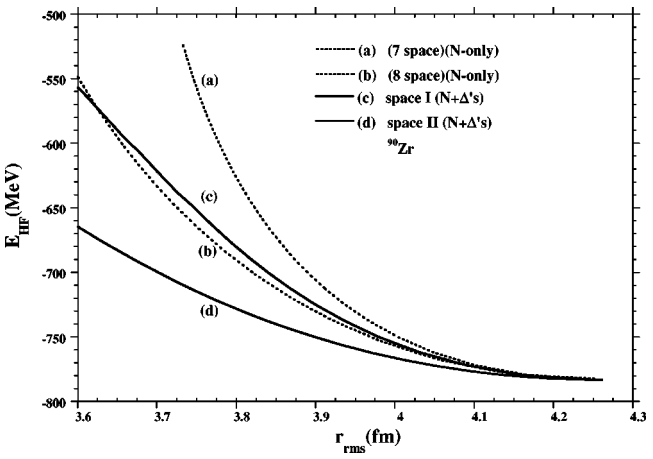

FIG. 1. Constrained spherical Hartree-Fock (SHF) energy E_{HF} vs $r_{\rm rms}$ for ^{90}Zr. Dotted lines correspond to the results of calculations performed in the nucleon-only model spaces, the 7 space and 8 space, respectively. Solid lines correspond to results obtained when Δ excitations are included: (c) the 7 space with Δ excitations restricted to the eight Δ orbitals $0S_{3/2}$, $0P_{1/2}$, $0P_{3/2}$, $0P_{5/2}$, $1S_{3/2}$, $1P_{1/2}$, $1P_{3/2}$, and $1P_{5/2}$; (d) the 8 space with Δ excitations restricted to the 16 Δ orbitals $0S_{3/2}$, $0P_{1/2}$, $0P_{3/2}$, $0P_{5/2}$, $1S_{3/2}$, $1P_{1/2}$, $1P_{3/2}$, $1P_{5/2}$, $0D_{1/2}$, $0D_{3/2}$, $0D_{5/2}$, $0D_{7/2}$, $0F_{3/2}$, $0F_{5/2}$, $0F_{7/2}$, and $0F_{9/2}$.

four different model spaces. On the other hand, the E_{HF} calculated with a much larger compression decreases as the size of the model space increases for either the N-only case (''7 space'' and ''8 space'') or the case including both N and Δ (space I and space II). For example, at $r_{\rm rms}=3.75$ fm (the nuclear volume is reduced by 32% from its ground state volume), there is a decrease of 108 MeV when the size of the N-only model space has expanded from ''7 space'' to ''8 space'' [curves (a) and (b)]. A similar change is also seen in the results from the calculations using a model space including both N and Δ [curves (c) and (d)]. By comparing (a) and (c) [or (b) and (d)], we see that the inclusion of Δ orbitals tends to decrease E_{HF} for compressed nuclei. The role of the Δ's is less significant as the $r_{\rm rms}$ approaches the ground state value.

One can understand these results by examining the excitation energies. For example, we find that it ''costs'' about 227 MeV, 119 MeV, 134 MeV, and 69 MeV of excitation energy to achieve a 32% volume reduction using the 7 space, 8 space, space I, and space II, respectively. This means that the static compression modulus is significantly reduced by adding the eight Δ orbitals to the 7 space. A comparable reduction in the static compression modulus is achieved when the size of the model space has expanded from the 7 space to the 8 space. The smallest values of the static compression modulus are achieved in space II, the largest of our model spaces combining nucleons and Δ's.

One may conclude from the above results the following: Increasing the size of the model space and including of the Δ resonances, together, induces a significant softening of the nuclear equation of state at large compression. While the qualitative nature of this conclusion is easy to understand, the quantitative behavior is quite striking. It is desirable to

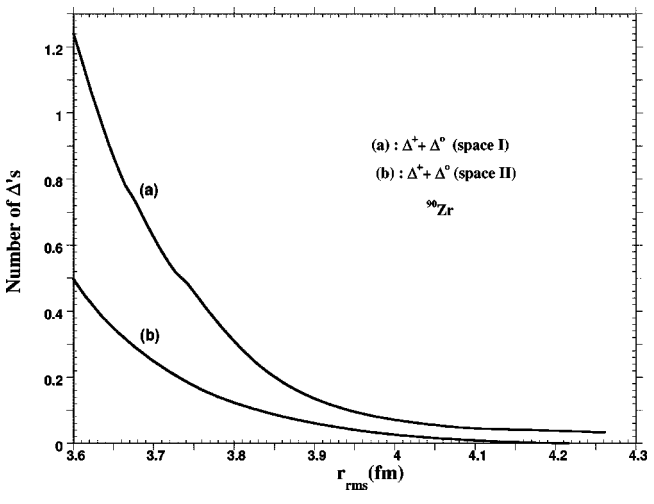

FIG. 2. Number of Δ's vs r_{rms} under compression for ^{90}Zr. The results of these calculations are performed in a model space of (a) space I as described in the text and (b) space II as described in the text.

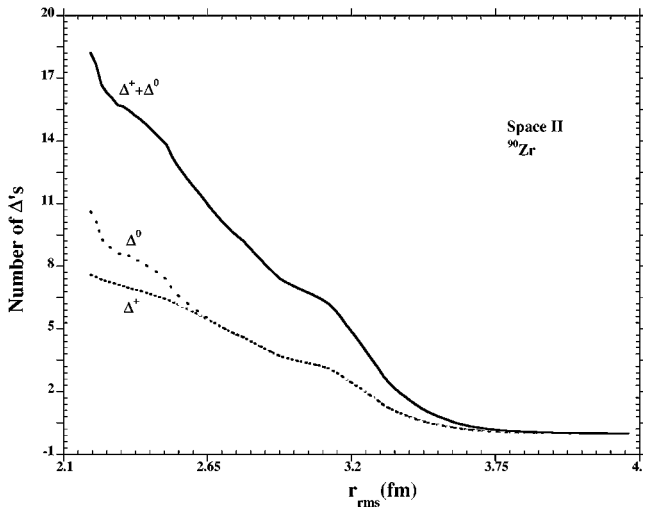

FIG. 3. Number of Δ's vs r_{rms} under compression for ^{90}Zr. The model space used is the one for curve (d) of Fig. 1. Dotted, dashed, and solid lines correspond to the number of Δ^+, Δ^0, and $\Delta^+ + \Delta^0$ created, respectively.

further investigate this model dependence of our predictions by considering larger model spaces. This is, however, a rather nontrivial numerical task and is beyond the scope of this paper.

In the models defined within space I and space II, the nuclei will have Δ components. It is interesting to see how the Δ components vary as nuclei are compressed. This is shown in Fig. 2. As expected, the number of the Δ's increases as the nuclear volume decreases. It appears that space I generates more Δ's than space II at fixed compression. This trend may be understood as a consequence of the expansion of the nucleon space which allows the nucleons to accommodate more easily the compressive load and hence the tendency to convert to Δ's is reduced.

To further explore how the Δ components vary under the compression of nuclei, we also have performed calculations in the region where the nuclear volume is reduced by as much as about 3/4 or more of its size at equilibrium. Clearly this is a very exploratory study since the considered space II is perhaps much too small for describing such dense nuclear systems. Nevertheless, the results can shed some light on the Δ dynamics at high densities accessible to relativistic heavy-ion collisions. The predicted numbers of Δ's as a function of r_{rms} are shown in Fig. 3. We see that the number of the created Δ's increases sharply with compression. For example, reducing the nuclear volume by about 72% ($r_{\mathrm{rms}} \sim 2.65$ fm) increases the percentage of the Δ's to about 10% of the baryons. By an additional 14% volume reduction, such that the resulting volume ($r_{\mathrm{rms}} \sim 2.2$ fm) is now only 14% of the original volume, the Δ population is almost doubled. It is interesting to note in Fig. 3 that the number of Δ^0's and Δ^+'s are the same until compression achieves about an 80% nuclear volume reduction. At that stage, the creation of Δ^0's becomes more favorable as the compression continues.

From the results shown in Figs. 1–3, one can draw several conclusions. First, space I produces a greater responsiveness in generating the Δ's at fixed compression than space II. Second, the static compression modulus is reduced significantly by enlarging the nucleon model space. Third, when moving to larger compression, including the Δ states reduces the static compression modulus even further, but their role in reducing the static modulus is less dramatic than enlarging the size of the nucleon model space. Fourth, the role of the Δ states in reducing the static compression modulus is larger in space I than in space II. The last result is consistent with the findings reported in Ref. [6].

We now turn to discussing the results for ^{100}Sn. These results are compared where possible with those of Ref. [7]. In the calculations of Ref. [7], the *G*-matrix elements for the *NN* interactions were based on the RSC potential [17] and the transitions to the Δ channels are described only by the transition potentials taken from Ref. [11]. On the other hand, the results in the present study are obtained using a much larger model space (space II). The *G*-matrix elements for the *NN* interactions are based on the Nijmegen potential [16], and the *G*-matrix elements associated with the Δ's are obtained from a coupled channel method developed in Ref. [12].

The predicted Hartree-Fock energies E_{HF} for ^{100}Sn as a function of the mean radius r_{rms} are displayed in Fig. 4. The differences between (a) and (b) indicate the changes due to the inclusion of the Δ in the model space with 26 nucleon states (7 space) and eight Δ states. Clearly the Δ degree of freedom tends to give more binding and soften the equation of state. Similar but weaker softening effects are also seen from comparing (c) and (d) which were obtained from calculations using a larger model space with 36 nucleon states (8 space) and 16 Δ states. All calculations give the same E_{HF} in the region near the equilibrium volume ($r_{\mathrm{rms}} \sim 5.1$ fm). This is consistent with the results shown in Fig. 1 for ^{90}Zr.

Figure 5 shows the predicted dependence of the number of the Δ's on the mean radius r_{rms} of ^{100}Sn. The results from Ref. [7] (dotted curve) are also shown for comparison. At equilibrium ($r_{\mathrm{rms}} \sim 5.1$ fm) we find that both calculations

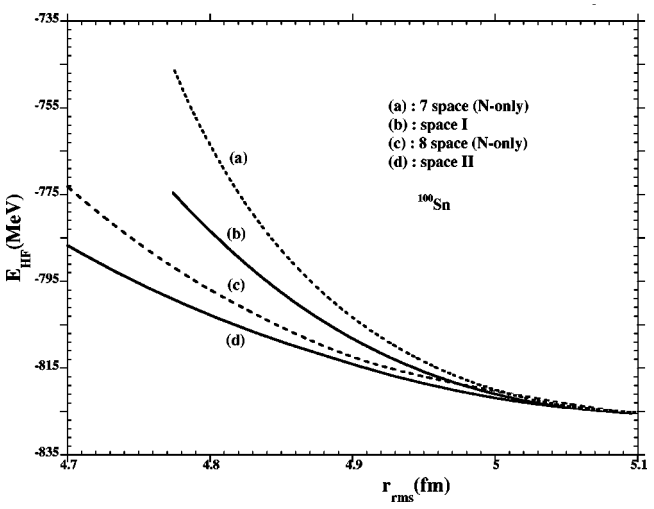

FIG. 4. Constrained SHF energy E_{HF} vs r_{rms} for ^{100}Sn. Lines with the labels (a), (b), (c), and (d) represent the results of calculations performed in various model spaces as indicated in the label and described in the text. Solid (dashed) line corresponds to $N+\Delta$'s (N-only).

yield no Δ's. However, they have rather a different dependence on the r_{rms}. We find that this difference in the r_{rms} dependence is mainly due to the change in model spaces, rather than to the change in effective NN and $N\Delta$ interactions. The larger model space (solid curve, space II) obviously gives a softer equation of state at high densities.

Figure 6 shows that the number of created Δ's increases sharply if we further compress ^{100}Sn to a volume of about half of its equilibrium size. However, at this nuclear density, which is twice the normal nuclear density, the percentage of nucleons converted to Δ's is only about 6% in ^{100}Sn. This result is consistent with our previous results [5] and with the information extracted from the data of relativistic heavy-ion collisions [1,2]. We also note that the numbers of Δ^+'s and

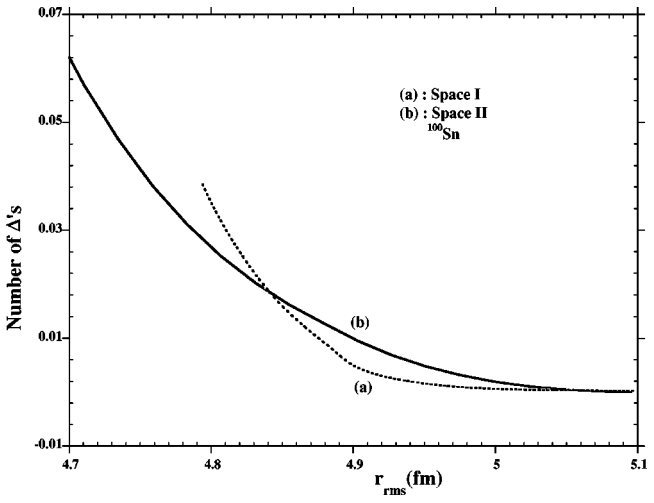

FIG. 5. Number of Δ's vs r_{rms} under compression for ^{100}Sn. Lines with the labels (a) and (b) represent the results of calculations performed in the space I and space II, respectively, as described in the text.

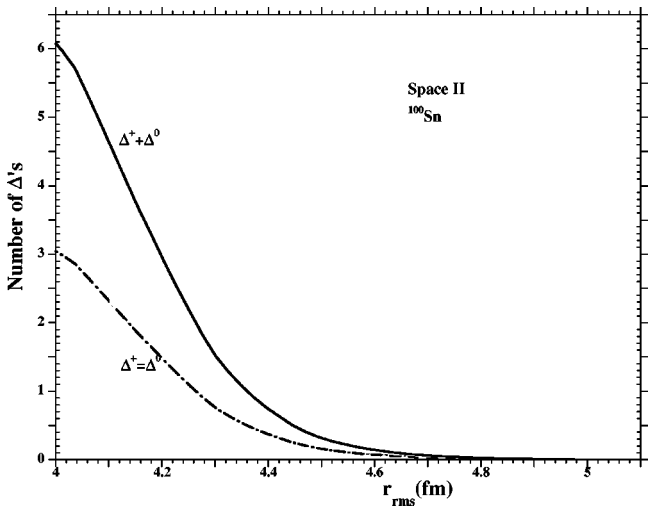

FIG. 6. Number of Δ^+, Δ^0, and $\Delta^+ + \Delta^0$ vs r_{rms} under compression for ^{100}Sn for the entire range of compression examined. The model space used is the one of curve (d) in Fig. 1.

Δ^0's are equal at all r_{rms} values examined here.

The density distributions of ^{100}Sn evaluated at equilibrium ($r_{\mathrm{rms}}=5.1$ fm) and at an about 20% reduced volume ($r_{\mathrm{rms}}=4.75$ fm) are compared in Fig. 7. Comparing curves c and c', we observe that the 20% reduction of nuclear volume greatly enhances the total density in the interior of the nucleus. Accordingly, the density is decreased with compression for the $r>5.63$ fm region. Similar situations are also observed for proton (neutron) densities if we compare curves b and b' (a and a'). The Δ density (curve d') for the 20%-compressed volume has a rather different distribution. It is peaked at a larger distance from the nuclear center. At equilibrium, the predicted Δ component is almost zero and hence is not shown in Fig. 7.

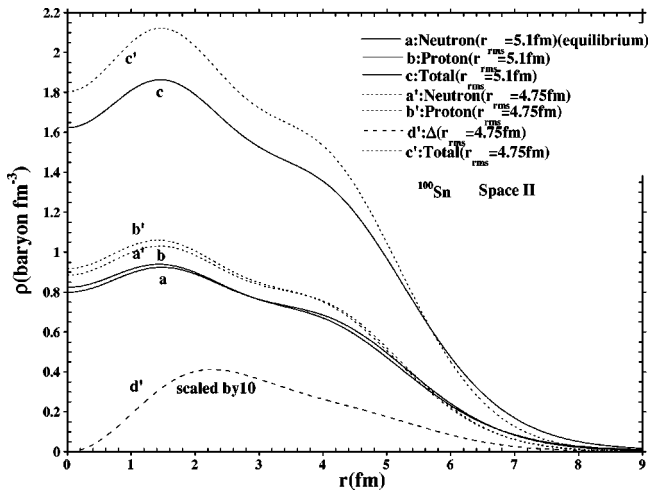

FIG. 7. Radial density distribution vs r for ^{100}Sn at $r_{\mathrm{rms}}=5.1$ fm (equilibrium) (solid lines) and 4.75 fm (dotted lines). Lines labeled with a and a' correspond to neutrons; b and b' correspond to protons; d' corresponds to Δ's while lines labeled with c and c' correspond to total radial density at these r_{rms} radii, respectively.

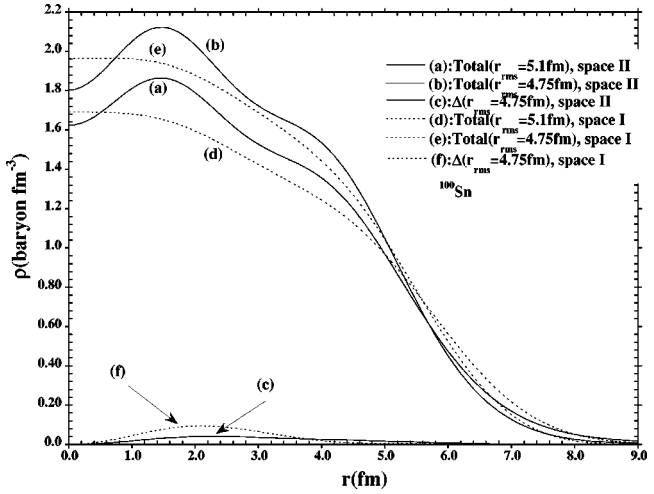

FIG. 8. Radial density distribution vs r for ^{100}Sn. Dashed (solid) lines represent results of calculations performed in the model space called space I (space II) in the text. Lines labeled (a) and (b) correspond to (a) total radial density at $r_{\rm rms}=5.1$ fm (equilibrium) and (b) total radial density at $r_{\rm rms}=4.75$ fm. Lines labeled (d) and (e) correspond to (d) total radial density at $r_{\rm rms}=5.1$ fm (equilibrium) and (e) total radial density at $r_{\rm rms}=4.77$ fm. Lines labeled (c) and (f) correspond to the Δ density at (c) $r_{\rm rms}=4.75$ fm and (f) $r_{\rm rms}=4.77$ fm, respectively.

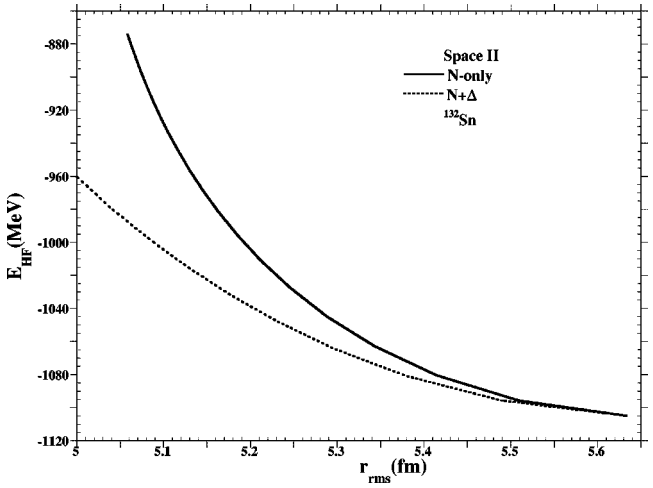

FIG. 9. Constrained SHF energy E_{HF} vs $r_{\rm rms}$ for ^{132}Sn. The full model space of both nucleons and Δ's is referred to as space II in the text. The solid line represents the result of calculations performed for nucleons only (also called the 8 space) while the dotted line presents the full space II result.

In Fig. 8 we compare the densities calculated in this work (space II, solid curves) and those in Ref. [7] (space I, dashed curves). By comparing the curves *a* and *d*, we see that the predicted shapes of the total densities in the region near the nuclear center are rather different for the nuclear volume at equilibrium ($r_{\rm rms}=5.1$ fm). This is also the case (curves *b* and *e*) at 20%-reduced volume ($r_{\rm rms}=4.75$ fm). The oscillating behavior of space II calculation (solid curves) is rather striking. In the lower part of Fig. 8, we see that the predicted Δ distributions at $r_{\rm rms}=5.1$ and 4.75 fm have rather different magnitudes while their shapes are very similar.

In Ref. [8] we have examined the effects due to adding more neutrons to the nucleus. Here we address the same issue by performing calculations for ^{132}Sn which has a large neutron excess over ^{100}Sn. Qualitatively, we find that the results for ^{132}Sn are similar to those presented in Figs. 4–8 for ^{100}Sn. For completeness, we show the predicted E_{HF}, number of Δ's, and densities for ^{132}Sn in Figs. 9–11.

By comparing the solid and dotted curves in Fig. 9, we see again that the Δ degree of freedom induces a considerable reduction in the compressibility along with a softer equation of state.

Figure 10 displays the dependence of the number of Δ's on the mean radius $r_{\rm rms}$ of ^{132}Sn. The results from using space I and space II are compared. We see that the predicted Δ population depends on the size of model space, similar to what we have observed in Fig. 2 for ^{90}Zr and Fig. 5 for ^{100}Sn. For both cases shown in Fig. 10, the number of Δ^0's is larger than the number of Δ^+'s at all radii during compression.

The predicted densities for ^{132}Sn are shown in Fig. 11. Similar to the pattern seen in Fig. 7, all densities near the center of the nucleus are greatly enhanced by compression. It is interesting to note that the oscillating behavior is reduced for the neutron density compared with the proton density and also reduced compared to the ^{100}Sn neutron density in Fig. 7.

In summary, we have investigated the ground state properties of ^{90}Zr, ^{100}Sn, and ^{132}Sn at equilibrium and at large compressions. A realistic effective Hamiltonian that includes NN, $N\Delta$, and $\Delta\Delta$ interactions is used. We have performed calculations in no-core model spaces within the framework of the CSHF approximation. The focus of our investigation is on the sensitivity of our predictions to the sizes of the nucleon and Δ model spaces. Our main findings are the following. The Δ degrees of freedom tend to soften the equation of state. The precise percentage of the Δ components at a specified compression depend on the size of the model space. At equilibrium, we find no case of mixing between

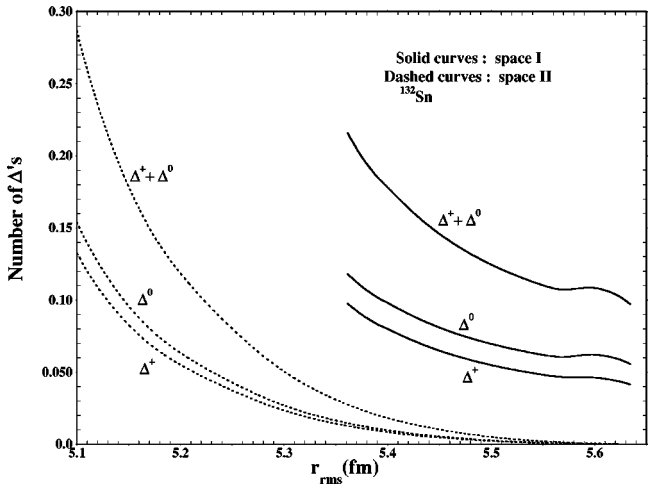

FIG. 10. Number of Δ^+, Δ^0, and $\Delta^+ + \Delta^0$ vs $r_{\rm rms}$ under compression for ^{132}Sn. The model spaces that are used are the ones of Fig. 5. Solid (dotted) lines represent results of calculations performed in space I (space II).

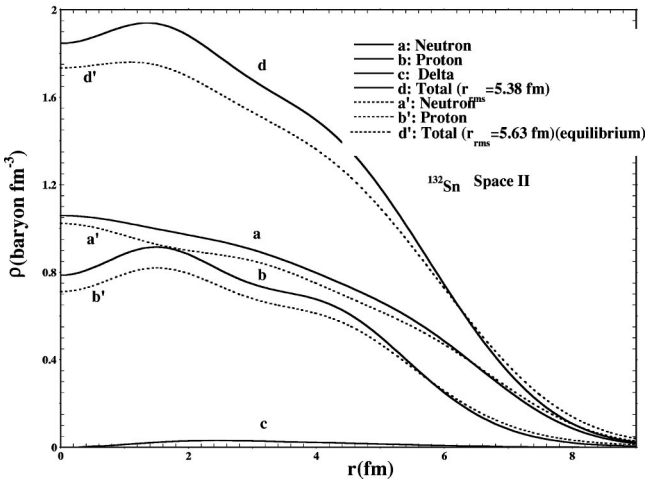

FIG. 11. Radial density distribution vs r for ^{132}Sn at $r_{\mathrm{rms}} = 5.63$ fm (equilibrium) (dotted lines) and 5.38 fm (solid lines). Lines labeled with a and a' correspond to neutrons; b and b' correspond to protons; c correspond to Δ's while lines labeled with d and d' correspond to the total radial density at these r_{rms} radii, respectively.

nucleons and Δ's in our largest model space of eight major nucleon shells plus 16 Δ orbitals. On the contrary, there is mixing in ^{90}Zr, and ^{132}Sn in the smaller model space of seven major nucleon shells plus eight Δ orbitals. Expanding the nucleon model space has a larger effect on reducing the static compression modulus and softening the nuclear equation of state than increasing the number of the Δ states in the cases we examined. Under extreme compression, at a density 2–3 times the normal nuclear density, the excitation of nucleons to Δ's increases sharply up to 10% of the total number of constituents.

To end this paper, we must note that our predictions depend rather strongly on the size of the chosen model space, especially at larger compression. This happens in spite of our adjustments to the effective Hamiltonian where we match the experimental ground state properties in each model space. Thus the results presented here should be viewed as first-stage qualitative indications of the role of the Δ degree of freedom in the compressed nuclei. The results also serve to motivate efforts with yet larger model spaces. In the future, we will both enlarge the model space further and solve for the corresponding model-space-dependent effective Hamiltonians from microscopic theory in order to make more quantitative predictions for analyzing the data of Δ production in relativistic heavy-ion collisions.

ACKNOWLEDGMENTS

We acknowledge support for this work from U.S. DOE Grant No. DE-FG02-87ER40371, U.S. DOE Contract No. W-31-109-ENG-38 and NSF Contract No. INT00-80491.

[1] U. Mosel and V. Metag, Nucl. Phys. News **3**, 25 (1993).
[2] L. Xiong, Z. G. Wu, C. M. Ko, and J. Q. Wu, Nucl. Phys. **A512**, 773 (1990); M. Hoffmann *et al.*, Phys. Rev. C **51**, 2095 (1995).
[3] E. A. Pasyuk, C. L. Morris, J. L. Ullmann, J. D. Zumbro, L. W. Kwok, J. L. Mathews, and Y. Tan, Acta Phys. Pol. B **29**, 2335 (1998).
[4] C. L. Morris, J. D. Zumbro, J. A. McGill, S. J. Seestrom, R. M. Whitten, C. M. Reidel, A. L. Williams, M. R. Braunstein, M. D. Kohler, and B. J. Kriss, Phys. Lett. B **419**, 25 (1998).
[5] M. A. Hasan, T.-S. H. Lee, and J. P. Vary, Phys. Rev. C **56**, 3063 (1997).
[6] M. A. Hasan, S. H. Kohler, and J. P. Vary, Phys. Rev. C **36**, R2180 (1987); **36**, 2649 (1987); J. P. Vary and M. A. Hasan, Phys. Rep. **242**, 139 (1994); Nucl. Phys. **A570**, 355 (1994); M. A. Hasan and J. P. Vary, Phys. Rev. C **50**, 202 (1994); **54**, 3035 (1996).
[7] M. A. Hasan, Ph.D. thesis, University of Jordan, 1995, Vol. 22, p. 777.
[8] M. A. Hasan, J. P. Vary, and T.-S. H. Lee, Phys. Rev. C **61**, 014301 (1999).
[9] B. H. Brandow, Rev. Mod. Phys. **39**, 77 (1967).
[10] K. A. Brueckner, Phys. Rev. **97**, 1353 (1955).
[11] M. Gari, G. Niephaus, and B. Sommer, Phys. Rev. C **23**, 504 (1981).
[12] Y. Tzeng, T. T. S. Kuo, and T.-S. H. Lee, Phys. Scr. **53**, 300 (1996).
[13] T.-S. H. Lee, Phys. Rev. Lett. **20**, 1571 (1983); Phys. Rev. C **29**, 195 (1994).
[14] T.-S. H. Lee and A. Matsuyama, Phys. Rev. C **32**, 516 (1985); **36**, 1459 (1987).
[15] A. Matsuyama and T.-S. H. Lee, Phys. Rev. C **34**, 1900 (1986); Nucl. Phys. **A526**, 547 (1991).
[16] V. G. J. Stoks, R. A. M. Klomp, C. P. F. Terheggen, and J. J. deSwart, Phys. Rev. C **49**, 2950 (1994).
[17] R. V. Reid, Ann. Phys. (N.Y.) **50**, 411 (1968).
[18] G. Bozzolo and J. P. Vary, Phys. Rev. Lett. **53**, 903 (1984); Phys. Rev. C **31**, 1909 (1985).
[19] L. Jagua, M. A. Hasan, J. P. Vary, and B. R. Barrett, Phys. Rev. C **46**, 2333 (1992).
[20] M. Saraceno, J. P. Vary, G. Bozzolo, and H. G. Miller, Phys. Rev. C **37**, 1267 (1988).